Putting a spin on it: amyloid aggregation from oligomers to fibrils

Zurlo, E.

4 In situ kinetic measurements of α-synuclein aggregation reveal large population of short-lived oligomers

Knowledge of the mechanisms of assembly of amyloid proteins into aggregates is of central importance in building an understanding of neurodegenerative disease. Given that oligomeric intermediates formed during the aggregation reaction are believed to be the major toxic species, methods to track such intermediates are clearly needed. Here we present a method, electron paramagnetic resonance (EPR), by which the amount of intermediates can be measured over the course of the aggregation, directly in the reacting solution, without the need for separation. We use this approach to investigate the aggregation of α-synuclein (αS), a synaptic protein implicated in Parkinson's disease and find a large population of oligomeric species. Our results show that these are primary oligomers, formed directly from monomeric species, rather than oligomers formed by secondary nucleation processes, and that they are short-lived, the majority of them dissociates rather than converts to fibrils. As demonstrated here, EPR offers the means to detect such short-lived intermediate species directly in situ. As it relies only on the change in size of the detected species, it will be applicable to a wide range of self-assembling systems, making accessible the kinetics of intermediates and thus allowing the determination of their rates of formation and conversion, key processes in the self-assembly reaction.

4.1 Introduction

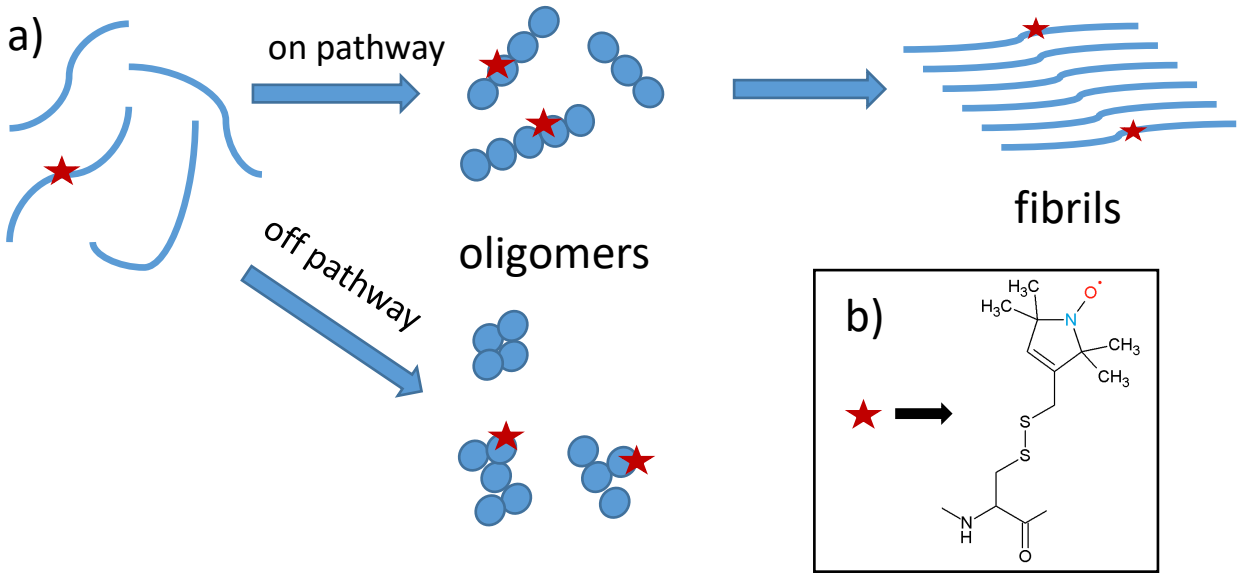

Figure 4.1 *a) Overall reaction pathways and intermediates of α-synuclein aggregation shown schematically. Blue spheres: monomers within oligomers (shapes of oligomers are arbitrary). Red stars: R1 nitroxide spin label (see b). b) Molecular structure of the R1 spin label attached to the protein.*

The function of the α-synuclein protein (αS) is associated with its ability to bind to the membranes of intracellular vesicles and thought to involve membrane remodeling and vesicle trafficking. It mainly localizes at the synaptic terminus where it plays a role in synaptic transmission.[134] The binding of αS to membranes may directly contribute to membrane remodeling by generating curvature or indirectly by acting as a non-conventional chaperone for the SNARE protein synaptobrevin.[135] Additionally the propensity of αS to connect vesicles plays a role in vesicle trafficking at the synapse by controlling the distal synaptic vesicle pool.[136]

While the exact functions of the αS protein only now start to become clear, its association with Parkinson's disease has been well documented. The in vitro aggregation of αS revealed that besides the cross-β fibrils, which represent the end-point of the amyloid aggregation, oligomers are also formed.[137–143] Several works have shown that these oligomeric species are toxic to cells[38,39], however, most studies rely either on fluorescently labelled αS species, use kinetically trapped oligomers which may not constitute intermediates of the aggregation reaction, or involve biochemically isolated oligomers and indirect detection. [144–147]

While these approaches are invaluable for structural and toxicological studies, they cannot detect the oligomers in situ, to reveal how the oligomers develop in the aggregating solution. Also labelling and isolation may cause a significant modification of the protein or oligomer structure. Thus, there is need for methods to detect such intermediates, directly in solution during the aggregation reaction, without the need for large fluorescence labels. Here we present an approach that closes this gap: In situ

continuous wave electron paramagnetic resonance (EPR). This method measures the rotational diffusion time of spin labelled objects in liquid solution at room temperature. Sensitivity of the EPR lineshape of nitroxide spin labels to time scales in the nano-second regime ensures that the aggregates of interest (see Figure 4.1) are well covered. To apply the method, the αS is labelled with the spin label shown in Figure 4.1b. This label is attached to a cysteine at position 56, which was introduced by site selective mutagenesis, resulting in the construct R1-αS, where R1 stands for the spin label. The spin label itself, see Figure 4.1b, is significantly smaller than commonly used fluorescent labels. The scarceness of unpaired electrons makes the method background free.

We use this methodology to reveal the appearance of an intermediate aggregated species. We present a kinetic model that explains the development of intermediates and fibrils.

4.2 Material and methods

4.2.1 Protein expression and labeling

Mutagenesis, protein expression and purification were performed as described previously.[148,149] The mutated protein was spin labeled following a standard protocol. The αS56 (cysteine mutant in position 56) was reduced with a six-fold molar excess per cysteine with DTT (1,4-dithio-D-threitol) for 30 minutes at room temperature. Removal of DTT was done by passing the samples twice through a Pierce Zeba 5 ml desalting columns. Immediately afterwards, a ten-fold molar excess of the MTSL spin label [(1-oxyl-2,2,5,5-tetramethylpyrroline-3-methyl)-methanethiosulfonate] was added (from a 25 mM stock solution in DMSO) and incubated for one hour in the dark at room temperature. After this, free spin label was removed by two additional desalting steps. Protein samples were applied onto Microcon YM-100 spin columns to remove any precipitated and/or oligomerised proteins and then diluted in buffer (10 mM Tris-HCl, pH 7.4). The initial protein concentration was 250 μM, the spin label concentration was 2.5 mM. Due to the high reactivity of the MTSL and the easily accessible cysteine, near stochiometric labeling was achieved under these conditions.[150] Samples were stored at -80 ^{0}C.

4.2.2 Sample preparation

Three aliquots of a stock solution of spin-labeled α-synuclein (concentration between 150 μM and 250 μM) were diluted in 1.5 mL of buffer each (10 mM Tris-HCl, pH 7.4), to a final concentration of 10 μM. The solutions also contained 90 μM wild-type α-synuclein for diamagnetic dilution. The experiments were carried out over five days. After an initial

measurement was taken at the time the spin-labelled protein was diluted (t = 0), the samples were allowed to aggregate in 2 mL Eppendorf tubes on a thermomixer (Eppendorf, Thermomixer comfort) with a speed of 1000 rpm at 37 ^{0}C. At each time point, 40 µL samples were drawn from the aggregation solution and kept in the fridge at 4 ^{0}C. From these, samples for EPR and Thioflavin T (ThT) fluorescence measurements were made. At the beginning samples were collected every 3 hours, at later times the intervals were longer (see text).

4.2.3 EPR measurement conditions

The 9 GHz, continuous-wave EPR spectra were recorded using an ELEXSYS E680 spectrometer (Bruker, Rheinstetten, Germany). The measurements were done under the following conditions: room temperature, a microwave power of 0.63 mW and a modulation amplitude of 0.25 mT at a modulation frequency of 100 kHz. The time expended on each measurement was adapted according to the spectral lineshape, i.e., the aggregation time, and they could last from 3 to 8 hours. Glass micropipettes of a volume of 50 µL (Blaubrand Intramark, Wertheim, Germany) were filled with 20 µL of the sample for each measurement. The spin concentration was determined by comparing the double integral of the EPR spectra with the double integral of a reference sample (MTSL, 100 µM). The spin concentrations were ≈ 10 µM for a total protein concentration of 100 µM.

4.2.4 Simulations of EPR spectra

MATLAB (version 9.4.0.813654, R2018a, The MathWorks, Inc., Natick, MA, USA) and the EasySpin package (5.2.4) were used for simulations of the EPR spectra.[48] The parameters of the simulation were manually adjusted to agree best with the experimental spectra. For all simulations, an isotropic rotation of the nitroxide ($S = 1/2$) was utilized. The following g-tensor values were used: g = [2.00906 2.00687 2.00300]. These values were obtained in previous experiments[151] and we used these values for the simulations presented here. The spectra were simulated with a superposition of four components: two fast fractions using the "Garlic" function and a medium and a slow fraction using the "Chili" function. The principal values of the ^{14}N hyperfine coupling tensor were $A_{xx} = A_{yy} = 13$ MHz and $A_{zz} = 110$ MHz. For the slow component $A_{zz} = 106$ MHz was used instead. A Gaussian component with a linewidth of 0.12 mT was used for all simulations. The spectrum obtained at t = 0 could be simulated with a single component, the fast fraction. The τ_r obtained at t = 0 was kept constant for all other simulations. From t = 3 hours a new component appeared, $\tau_r = 0.24$ ns which we attribute to free spin label. Its contribution to the spectra never exceeded 10 %. Optimal τ_r values of the medium and

slow components were derived from later time-point spectra and then kept constant for the entire series. For each time point, the relative contribution of the four components was optimized considering all time points.

4.2.5 Fitting of kinetics

The EPR measurements yield, after processing, the monomer-equivalent concentrations of monomers, intermediates and fibrils at different time points. We fit a minimal model of the aggregation of αS into fibrils that additionally includes the formation of oligomers of size n directly from monomers with rate constant k_o. Oligomer dissociation proceeds at rate constant k_d. Oligomers can be converted to fibrils by rate constant k_c. Fibrils grow by addition of monomers to their ends with rate constants k_+ and we allow for the presence of secondary processes, i.e. the possibility of fibrils to multiply in a monomer-independent manner, e.g. by fragmentation, by rate constant k_2. We do not include oligomeric species formed by a secondary process. More detailed descriptions of these kinetic models can be found for example in Meisl et al.[152–154]

Invoking conservation of mass, $m_{tot} = m(t) + M(t) + O(t)$, the aggregation process can be described by the following set of differential equations:

$$P'(t) = k_c\, O(t) + k_2\left(\mathrm{m_{tot}} - n\, O(\mathrm{t}) - m(t)\right)$$

$$M'(t) = 2k_+ P(t) m(t)$$

$$m'(t) = -2\, k_+ P(t) m(t) - n k_o m(t)^n + n\, k_d O(t)$$

$$O'(t) = k_o m(t)^n - (k_c + k_d) O(t)$$

Where $M(t)$ is the monomer-equivalent concentration of fibrils, $P(t)$ and $O(t)$ are the number concentrations of fibrils and of oligomers, respectively and $m(t)$ is the free monomer concentration. These equations were numerically integrated and fitted to the data by least squares minimization. We assumed a monomer-concentration independent secondary mechanism, such as fragmentation, based on previous studies of αS[155] aggregation into amyloid fibrils and the fact that vigorous shaking tends to induce fragmentation[156]. Additionally, given that the experiments were only recorded at a single initial monomer concentration, they do not provide strong constraints on the reaction orders[154]. The data provide constraints for a number of parameters: oligomers are in fast equilibrium with monomers, thus the equilibrium constant, k_o/k_d can be determined accurately but only an approximate lower bound can be given for the individual rates (corresponding to the requirement that the oligomerization reaction proceed fast enough to be in effective equilibrium relative to monomer depletion). Equally, the rates of elongation, the secondary process and conversion are interdependent (as is the case in all unseeded aggregation reactions) and thus only the products k_+k_c and k_+k_2 can be

constrained. Finally, the data show only a weak dependence on the reaction order of the oligomerization reaction, *n*.

4.3 Results

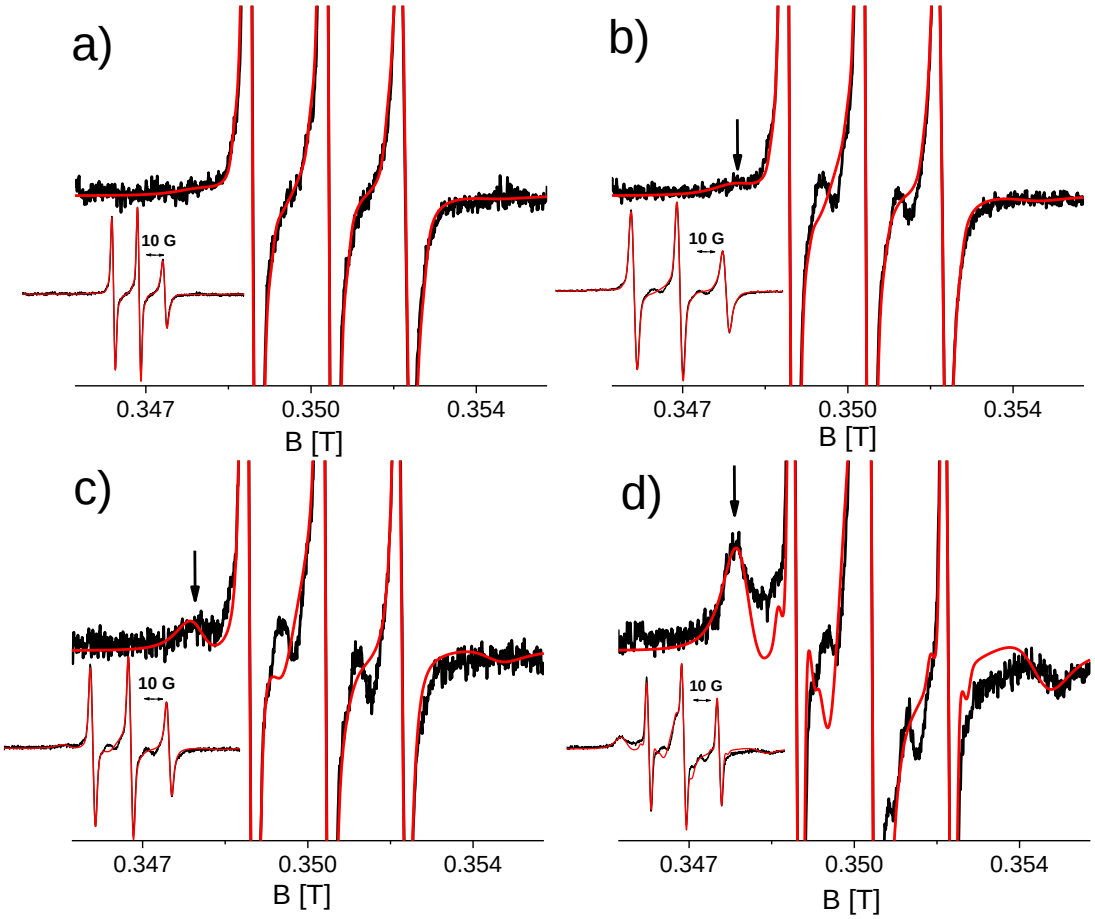

Figure 4.2 *Room temperature EPR spectra of α-synuclein at different time points of aggregation. Full spectra: Inset. Zoomed-in spectra: Amplitude expanded four-fold with respect to inset. a) Start of aggregation (t = 0). b) 9 hours of aggregation. c) 24 hours of aggregation. d) 42 hours of aggregation. Black: Experimental spectra. Red: Simulated spectra. Arrow: feature of broad spectral component (see text).*

The aggregation of 100μM α-synuclein was monitored at pH 7.4 and 37 ^{0}C under rapid shaking (1000 rpm), over the course of 120 hours. Figure 4.2 shows the development of the EPR spectra of R1-αS over time for four selected time points. The spectra at the start of the aggregation and after nine hours of aggregation (9 h) are dominated by the three narrow lines typical of nitroxides in fast rotational motion.

Starting at nine hours a new component with a broader linewidth (marked by an arrow) develops, that increases in amplitude with time. Its lineshape is due to a nitroxide with a slower rotation and shows that a fraction of R1-αS becomes more immobilized as the

aggregation progresses. Line broadening by spin-spin interaction can be excluded, because the R1-αS was diluted in a 1 : 9 ratio with wt-αS, which increases the distance between the spins of the nitroxides sufficiently to suppress spectral effects of their interaction (diamagnetic dilution).

Table 4.1 *Rotation correlation time (τ_r) of R1-αS in the three fractions observed by EPR.*

	fast	medium	slow
τ_r (ns)	0.40	4.00	10

By spectral simulation[48] three components can be extracted, referred to as the fast, medium and slow components. Their respective rotation correlation times (τ_r) are given in Tab. 4.1, and their lineshape is shown in Figure S4.2. The τ_r value of the fast fraction agrees with the τ_r values of monomeric αS with the spin label at the position of R1- αS.[157] The amount by which each fraction contributes to the spectra is shown in Figure 4.3.

The magnitude of τ_r relates to the size of the aggregated species, where, qualitatively, a longer τ_r corresponds to a larger species, see for example M. Hashemi Shabestari et al.[65]. Therefore, the medium fraction can be attributed to smaller aggregates than the slow fraction.

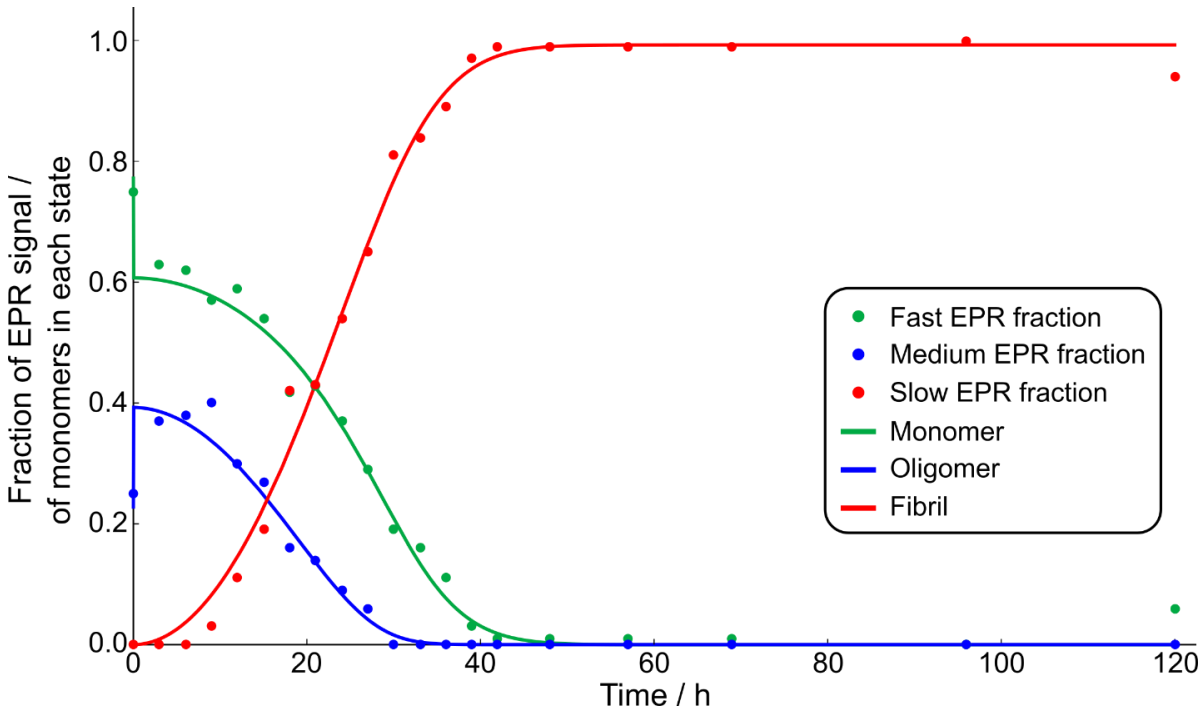

Figure 4.3 *Aggregation of α-synuclein as a function of time derived from EPR. Amount of fast fraction (green dots) caused by monomers. Amount of medium fraction (blue dots) assigned to oligomers. Amount of slow fraction (red dots) assigned to fibrils. The solid lines are the fractions of monomer, oligomer and fibrils predicted from the best fit of the model, with an oligomer size of n=3.*

The fast component decays to zero within the first 40 hours. The medium fraction increases to a maximum value of 40 % within the first 10 hours and then decays. At 30 hours, this component has fully decayed. The medium fraction disappears before the monomer fraction is depleted. The slow fraction appears after 12 hours, it increases to reach 100 % at 40 hours, and then remains at its plateau level until the end of the measurements, at 120 hours.

The kinetics of monomer, fibrillar and oligomeric fractions determined in this way were used in a kinetic analysis to determine the mechanism of aggregation and the respective reaction rates. The minimal model that was able to describe the data included an oligomeric species, formed directly from monomer, that can convert to growth-competent fibrils in a unimolecular reaction. Fibrils grow by addition of monomer and existing fibrils can lead to the formation of new fibrils via a secondary process, but they do not significantly affect the production of oligomers.

4.4 Discussion

Methods to determine the time course of amyloid aggregation are important as intermediates of aggregation are believed to be key toxic species[38,39,158–160]. Here we focus on αS, an amyloid protein related to Parkinson's disease, whose physiological role is yet to be determined.

Under the conditions investigated here, αS is expected to fibrilize slowly, i.e. over the course of days. We track the aggregation of α-synuclein in situ by EPR lineshape changes, which reflect the mobility of the spin label in R1-αS.

Following the time course of the process over the period of 5 days, three distinct fractions are observed: A fast fraction is due to monomeric R1-αS. The fast fraction decays with time and at 40 hours has disappeared. The second fraction, with medium mobility, grows with time with a maximum early in the aggregation reaction followed by a decay. The transientness of this species suggests that this fraction represents oligomers which are higher in energy than the fibrillar end product of the aggregation reaction. The slow fraction appears after a lag time and then grows to a plateau value that is close to the full population.

4.4.1 Relation of the EPR derived fractions to the aggregation state of αS

The contribution to the overall EPR signal reflects the relative number of αS proteins in this particular aggregation state. Thus, the fraction with a fast rotational correlation time

corresponds to the fraction of total αS that is in the monomeric state. This signal shows a decay over time as monomers are being converted into aggregates. In addition to the monomeric species, two types of aggregates can be distinguished by EPR, those with a slow rotational correlation time, corresponding to large aggregates and those with a medium rotational correlation time, corresponding to intermediate aggregate sizes. The time dependence (Figure 4.3) shows that intermediate-sized aggregates are formed initially, their time course closely resembling that of the monomer after the initial measurement. The larger aggregates are only formed at a later stage.

It is not possible to derive the exact size of the aggregate, because of the local mobility of the spin label, i.e. the rotation about the single bonds that link the pyrolidine ring to the protein backbone (Figure 4.1 b), see M. Hashemi Shabestari et al.[65] for a more detailed discussion. In the present context, a lower limit of the size of the aggregate can be estimated from the ratio of the τ_r values of the aggregates with respect to the monomer, showing that the medium fraction comprises minimally ten monomers, the slow fraction at least 25 monomers. We have discussed the factors entering such estimates in detail in M. Hashemi Shabestari et al.[65]

The exponential increase of ThT activity appears around 35 hours (Figure S4.1), consistent with the medium fraction consisting of non-fibrillar aggregates. The slight discrepancy between the appearance in time of the large aggregate fraction as measured by EPR and the ThT fluorescence (Figure S4.1) is likely due to the poor sensitivity of ThT for structures with less beta-sheet content (see SI). Thus, we will refer to the medium fraction as oligomeric and the slow fraction as fibrillar.

Based on these observations we propose the following reaction scheme: Oligomers of size n form directly from monomers with rate constant k_o and dissociate with rate constant k_d. They can be converted to fibrils by rate constant k_c. Fibrils in turn grow by addition of monomers to their ends with rate constants k_+ and we allow for the presence of a monomer-concentration independent secondary process, such as fibril fragmentation, by rate constant k_2. Based on the EPR data, the oligomeric species appear to be in fast equilibrium with monomers on the timescale of the aggregation reaction. Indeed, we find that the rates of oligomer formation and dissociation are fast with $k_d > 1$ h^{-1} and only their equilibrium ratio being well constrained. Therefore, monomeric and oligomeric species should be considered part of the same ensemble of reactants for the purposes of a kinetic description. In other words, whether new fibrils are formed directly from monomers or by conversion of oligomeric intermediates is thus not distinguishable based on these kinetic measurements alone. The data are best fit by an oligomer reaction order of $n = 3$ (see Figure 4.3), but the dependence of the goodness of fits on this reaction order is weak, and reasonable fits can be achieved also with $n = 10$, the lower limit predicted for the oligomer size based on our EPR data alone (see Figure S4.3). It is worth noting that a kinetic analysis as presented here yields reaction orders, rather than oligomer sizes directly. In the simplest interpretation, i.e. when the reaction modelled is a single elementary step, the reaction order is equivalent to the oligomer size. However, in more

complex reactions, e.g. when heterogeneous nucleation on a surface is involved, reaction orders can be significantly smaller than the oligomer size. Assuming n =3, the best fit yields $k_d > 1$ h^{-1} and $k_o/k_d = 5.8x10^7$ M^{-2}, $k_+k_2 = 55$ $M^{-1}h^{-2}$ and $k_+k_c = 130$ $M^{-1}h^{-2}$. Note that only the combined rates of nucleation and elongation can be constrained; this is a result of the fact that measurements of the mass concentration of aggregates in the absence of seeds are determined only by a product of these rates, rather than the individual rates.[22] Typical elongation rates are on the order of 10^6 $M^{-1}h^{-1}$,[161] thus conversion, k_c, is likely to be orders of magnitude slower than dissociation, k_d. A key result is that the oligomers are formed directly from monomer, also in the absence of fibrils, and thus constitute primary oligomers, rather than secondary oligomers, i.e. they are potential intermediates of primary nucleation, not of secondary nucleation, as observed for example in the aggregation of Aβ42, one of the main proteins that aggregate in Alzheimer's disease. Furthermore, the fast oligomer dissociation rate compared to rate of conversion of oligomers into fibrils, as well as the fact that oligomers are in equilibrium with monomers, indicates that most oligomers dissociate before they can convert into fibrils. In Cremades et al.[10] two types of oligomers were identified, type A and type B. Type A oligomers are smaller and dissociate more readily than type B ones and both types dissociate more slowly than the oligomeric species we observe here. Thus, while the dynamics of the oligomer fraction observed here more closely resembles that of type A than type B oligomers of Cremades et al.[10], the majority of oligomers we detect do not appear to be present in single molecule experiments. While the different label may play a role, the fact that our technique requires neither dilution nor separation is likely to be the main source of the observed differences. Given our finding of a fast dissociation rate, we would expect the oligomeric species we detect here in-situ to dissociate significantly upon dilution, which is required to obtain single molecule data. The in-situ measurement by EPR allows us to detect these meta-stable species which are too short-lived to be measured by other techniques.

4.5 Conclusion

We have demonstrated the power of EPR to measure the presence of oligomeric species over the time course of the aggregation reaction, without need for dilution, size exclusion or other techniques that could potentially alter the size distribution. We find that a large population of non-ThT active intermediates from during the aggregation of αS at pH 7.4 and 37 ^{0}C. These oligomeric species are in fast exchange with the monomer pool and thus the data are consistent with them being intermediates on the primary nucleation pathway. They are not consistent with the detected species being secondary oligomers, i.e. formed via a process that is catalyzed by existing fibrils, which is believed to be the main source of oligomers during the aggregation of Aβ42. Oligomers are short lived on the timescale of the aggregation reaction and most disappear by dissociation, not by conversion to fibrils. We envision that this combination of non-disruptive oligomer

detection and kinetic analysis will be applicable to study the effect of a range of conditions on the oligomer formation reaction of αS and other amyloid forming proteins.

4.6 Supporting information

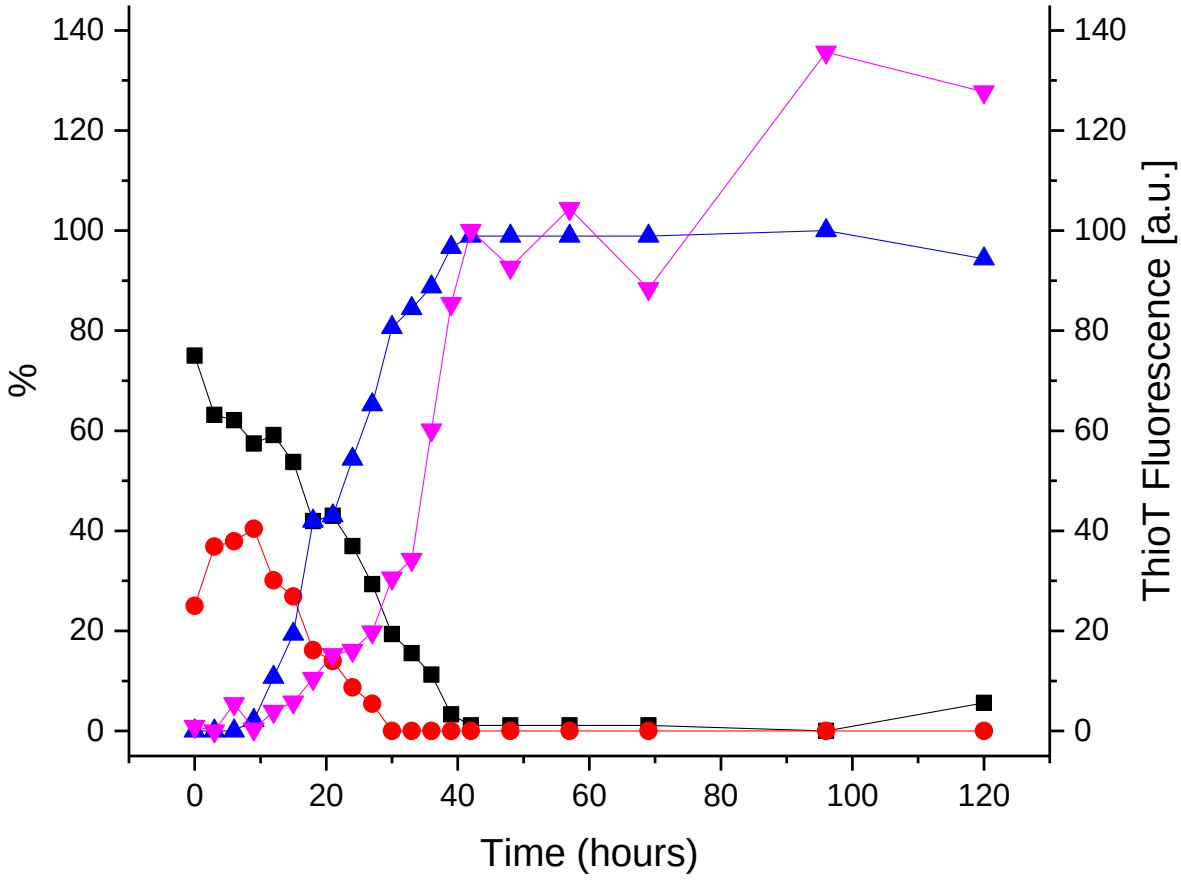

Figure S4.1 *Aggregation of α-synuclein as a function of time. Amount of fast fraction (black) caused by monomers. Amount of medium fraction (blue) assigned to oligomers. Amount of slow fraction (red) assigned to fibrils. Amount of fibrils derived from ThT fluorescence (pink, normalized to 100 at time 42 hours, the presumed plateau value). A 10 % component of free spin label was subtracted from the spectra from 3 to 120 hours. The lines are a guide to the eye.*

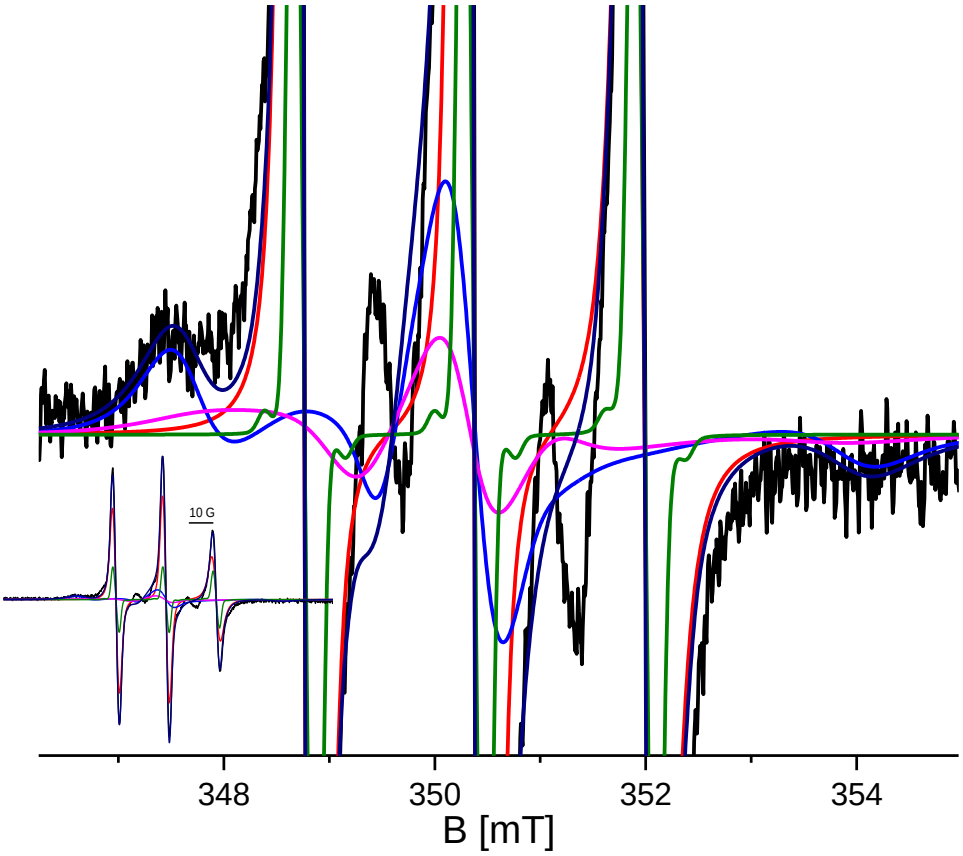

Figure S4.2 *Spectral components used in the simulation of the EPR spectra of α-synuclein (18 hours of aggregation). Full spectra: Inset. Zoomed-in spectra: Amplitude expanded ten-fold with respect to inset. Experimental spectra (black), fast component (red), medium component (pink), slow component (blue), free spin label (green). Total simulation (navy). For details see text.*

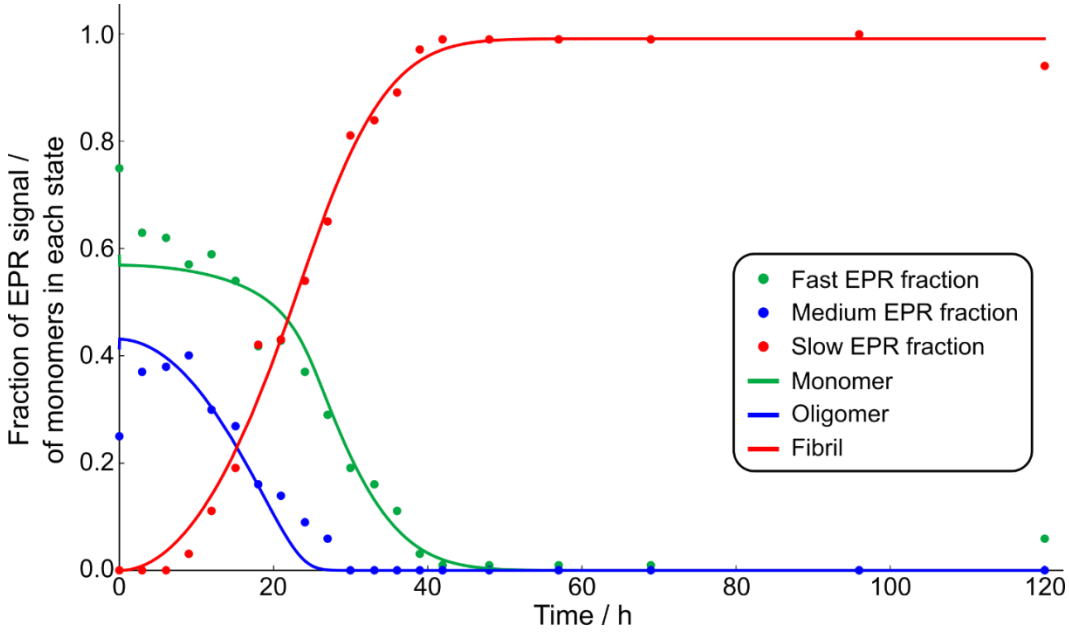

Figure S4.3 *Fits of the EPR data as in Figure 4.2, but with the oligomer size set to n=10.While the fibrils time course matches equally well with the data as for n=3, the fits to the monomer and oligomer populations are significantly worse.*